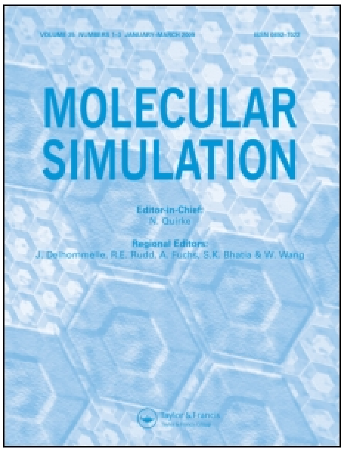

Molecular Simulation
Publication details, including instructions for authors and subscription information:
http://www.informaworld.com/smpp/title~content=t713644482

Effects of Local and Gradient-Corrected Density Approximations on the Prediction of the Intralayer Lattice Distance *c*, in Graphite and LiC_6

K. R. Kganyago[a]; P. E. Ngoepe[ab]
[a] Materials Modelling Center, University of the North, Sovenga, South Africa [b] Division of Materials Science and Technology, CSIR, Pretoria, South Africa

To cite this Article Kganyago, K. R. and Ngoepe, P. E.(1999) 'Effects of Local and Gradient-Corrected Density Approximations on the Prediction of the Intralayer Lattice Distance *c*, in Graphite and LiC_6', Molecular Simulation, 22: 1, 39 — 49

To link to this Article: DOI: 10.1080/08927029908022085

URL: http://dx.doi.org/10.1080/08927029908022085

Molecular Simulation, 1999, Vol. 22, pp. 39–49
Reprints available directly from the publisher
Photocopying permitted by license only

EFFECTS OF LOCAL AND GRADIENT-CORRECTED DENSITY APPROXIMATIONS ON THE PREDICTION OF THE INTRALAYER LATTICE DISTANCE c, IN GRAPHITE AND LiC_6

K. R. KGANYAGO[a] and P. E. NGOEPE[a,b,*]

[a] *Materials Modelling Center, University of the North, Sovenga, 0727, South Africa;*
[b] *Division of Materials Science and Technology, CSIR, PO Box 395, Pretoria, South Africa*

(Received October 1998; accepted November 1998)

Ab initio total energy calculations, on hexagonal models of graphite and LiC_6, are carried out within the most widely density functional theory (DFT) implementation, the local density approximation (LDA). Improvements to LDA in the form of generalized gradient approximation (GGA) are explored. Structural parameters predicted by LDA, as expected underestimate experiment within 1–2% margin of accuracy. GGA does not give a good account in the prediction of lattice parameter c, especially in graphite. This is evident in both recently implemented gradient corrections by Perdew and Wang and earlier corrections by Becke approximations. A substantial improvement is seen on introducing lithium ion in LiC_6 and using recent approximations. Valence electron densities from both LDA and GGA calculations, shows charge distribution plots that compare well with experimental results. Charge density distribution plots of these approximations appears similar on a larger scale.

Keywords: Graphite; LiC_6; LDA; GGA; structural; charge density

INTRODUCTION

Density functional theory [1] has provided a convenient first principle framework for studying the electronic and structural properties of a wide range of materials. In other classes of materials, systematic errors in density

---

*Corresponding author. e-mail: khomotso@technologist.com functional calculations have been reported. In particular difficulties are encountered in determining the form of the exchange correlation interaction, the local-density approximation [2] and the generalized-gradient approximation being the most common forms [3, 4]. Generalized gradient approximations were proposed for the correlation energy by Perdew [3] and for the ex-change energy by Perdew and Wang [3] and by Becke [4]. It is important to explore the limits of the density functional and of the LDA and GGA forms of the exchange-correlation functional in calculating crystalline solid.

We investigate the effect of the approximations to the gradient term of the LDA and GGA to structural and electronic properties of graphite and lithium intercalated graphite. The two materials are structurally simple and hence are amenable to both experimental and theoretical techniques. Furthermore, lithium-graphite intercalation compounds (Li–GICs) have recently drawn attention as safe alternative anode materials for rechargeable lithium battery [5]. Extensive experimental work on graphite and LiC_6 has been done relating to the equation of state, elastic constants and energy bands [6–16]. A study of these materials by *ab initio* methods has been undertaken since the 1980's. Each of these studies has focussed on structural, electronic and optical properties [16–25]. Recently charge density and charge transfer and how they affect inter and intra planar bonding have been shown [18, 24].

STRUCTURAL CONSIDERATION

The structure of graphite crystals was first proposed by Bernal in 1924. It belong to the space group with regularly stacked 2D hexagonal layers (graphenes) which are one atom thick. Graphite structure (see Fig. 1a) is characterized by strong covalent bond in the graphenes which are connected by weak van der Waal forces. In this structure (ABABA... stacking), two kinds of atoms, α and β, form the asymmetric unit. α-atoms have neighbours above and below them in adjacent layers, while β atoms are above and below the empty centers of the hexagonal rings in adjacent layers. The graphenes are rather widely separated, their distance being greater than twice the distance between two carbon atoms within the layers. Lithium intercalation into graphite is a process in which graphite accepts charged lithium ions between the graphenes. When lithium ion is introduced, there are structural changes that affect the crystallinity. For most stages (Li_xC_y) the graphenes assumes an AAAA... stacking with lithium sandwiched between them. LiC_6 assumes an $A\gamma A\gamma A\gamma A$... stacking pattern, where γ is

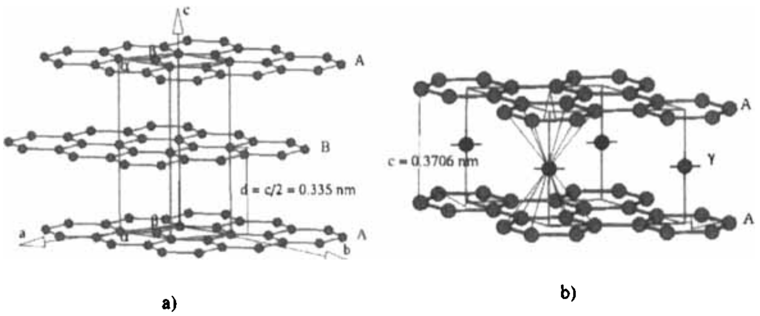

FIGURE 1 (a) Schematic drawing of the crystal structure of hexagonal graphite showing the AB layer stacking sequence and the unit cell. (b) Structure of Li-intercalated graphite compound LiC_6 (Stage 1) with the AγA stacking sequence, γ being the fictitious Li-ions layer midway the graphenes. (See Color Plate I).

the positions of the lithium ions (Fig. 1b). A complete charge transfer can take place when intercalated atoms are alkali metals such as lithium. When this happens, in general, the relatively weak van der Waals forces are replaced with stronger Coulomb interaction.

CALCULATIONS

Our calculations were performed using density functional technique (DFT) in both the local density approximation (LDA) and gradient-corrected LDA (GGA). LDA is known to underestimate bond lengths in molecules and cell parameters in crystals, while GGA typically remedies this shortcoming. However, there is much evidence that GGA is prone to overcorrect the LDA results in ionic system; it often overestimates cell parameters when LDA data is in good agreement with experiment. The work was carried out using Cambridge Sequential Total Energy Package (CASTEP) [26] and Planewave [27] codes. In the latter we used a preconditioned conjugate-gradient method to minimize the electronic degrees of freedom. The electronic wave functions were expanded in a plane-wave basis set with periodic boundary conditions. To test convergence with respect to the basis set size, calculations were performed at various kinetic energy cutoffs. It was determined that a cutoff of 33 Ha (~600 eV) was required for a satisfactory convergence of structural parameters. For each structure we calculated the ground state total energy over a wide range of volumes (lattice parameter $a = b$, for a constant value of c) and lattice constants a and c. We employed the nonlocal norm-conserving ionic pseudopotential of Troullier and Martins [28], for Li and C.

CASTEP employs special point integration over the Brillouin zone and a plane-wave basis for the expansion of the wavefunctions. Norm-conserving non-local pseudopotentials of the form suggested by Kleinmann and Bylander [29] were used. Cutoff energies of up to 600 eV and 900 eV were used for the expansion of the wavefunctions. Ceperly and Adler [30] using Monte Carlo techniques calculate the exchange-correlation energy function numerically for a large range of densities. An analytical fit to these results by Perdew and Zunger [31] is used in our calculation. A gradient-corrected form of the exchange-correction functional is used in the form suggested by White and Bird [32]. Fast Fourier transforms (FFT) sampling of special k-points was used to perform the integration in k-space over the first Brillouin zone. The minimum FFT grid of 18 × 18 × 50 and 32 × 32 × 27 for graphite and LiC_6, respectively, is sufficient for the cutoff energy of 900 eV. For the calculation in space group $P6_3/mmc$, 24 sampling k-points in the irreducible wedge of the Brillouin zone were used. Some calculations were also performed in space group P1 to check the results of the calculation with constrained symmetry. For the calculation in space group P6/mmm, 15 sampling k-points in the irreducible wedge of the Brillouin zone were used. The k-points were generated using the Monkhorst–Pack [33] scheme with parameters (9 × 9 × 4) and (5 × 5 × 6) for graphite and LiC_6 respectively. Each **k**-point was represented with an equivalent of 3650 and 3200 plane waves for graphite and LiC_6 respectively.

RESULTS ANALYSIS AND DISCUSSIONS

Structural Properties

The results of the equilibrium lattice parameters and bond lengths of graphite and LiC_6 are given in Table I. These were calculated both with LDA and GGA forms of the exchange correlation interaction, using Castep and Planewave codes. The equilibrium structure has been determined by relaxation with respect to a and c lattice parameters. We first considered $a = b$ lattice parameter with a fixed c. For graphite there is a tendency for LDA to underestimate a parameter and the C—C bond lengths, as is usually the case. This is clearly depicted by the Castep calculation, and Planewave has reproduced these values well. The inclusion of gradient corrections is supposed to increase the LDA parameters. As noted in Table I, GGA by Becke (Planewave) has overestimated the lattice parameter [6, 8, 17] and bond length, whereas that of Perdew and Wang (Castep)

TABLE I Resulting structural parameters of graphite and LiC$_6$

		$LDA_{planewave}$	LDA_{castep}	$GGA_{planewave}$	GGA_{castep}	*Experiment*
Graphite	a(Å)	2.460	2.450	2.480	2.440	2.460 [6]
	c(Å)	6.600	6.500	...	...	6.700
	V(Å)	–	34.175	...	33.893	35.100
	C—C bond length	1.420	1.415	1.432	1.409	1.420
LiC$_6$	a(Å)	4.400	4.300	4.400	4.300	4.305 [17]
	c(Å)	4.000	3.700	4.100	3.800	3.706
	V(Å)	–	59.073	–	–	59.481
	C—C bond length	1.552	1.430	1.463	1.440	1.441

has, contrary to expectations, underestimated both quantities. In the case of LiC$_6$, which is metallic, LDA and GGA (Castep) predict a lattice parameter accurately well. The parameter is overestimated by both approximations from Planewave calculations. This deviation could be partly ascribed to Planewave not being tailored to handle metallic systems. In general it may be concluded that a and b ($a = b$) parameters are reasonably reproduced by LDA and GGA calculations. As known, these parameters span a graphitic plane wherein, carbons are bonded together by strong covalent bonds (σ-bonds) from sp^2 hybridization.

A comparison of the c lattice parameter predictions, from both Castep and Planewave codes, by the two forms of exchange-correlation is enlightening. Table I shows that LDA (Castep) calculation underestimates this value in graphite. However, both Becke and Perdew and Wang GGAs, fail to predict the value of c, as noted from the variation of the total energy with cell parameter in Figure 2d. For LiC$_6$, predictions of c by LDA and GGA (Castep) calculations are close to experimental values. The intraplanar C—C bond lengths follow similar trends. The LDA and GGA (Planewave) overestimate the c parameter by ~8% and the discrepancy has been accounted for above. Hence, it may be concluded that the GGA form of the exchange-correlation appears to be inadequate in handling the weaker interlayer van der Waals bonds in graphite. It however approximates the interlayer bonding in LiC$_6$ better, which though weak is stronger than in graphite. Indeed previous studies [18] have shown that lithium ion in LiC$_6$ contribute charge to a π-density environment and thereby slightly increase interplanar bonding. Hence GGA, whose contribution is supposed to be short ranged, gives a more reasonable prediction of this bond in LiC$_6$.

The volumes were calculated for both systems using Castep within the local density approximation. This was done by first calculating the c/a ratio from the experimental parameters of both graphite (2.724) and LiC$_6$ (0.86). Structures of different volumes were then derived from this ratio and

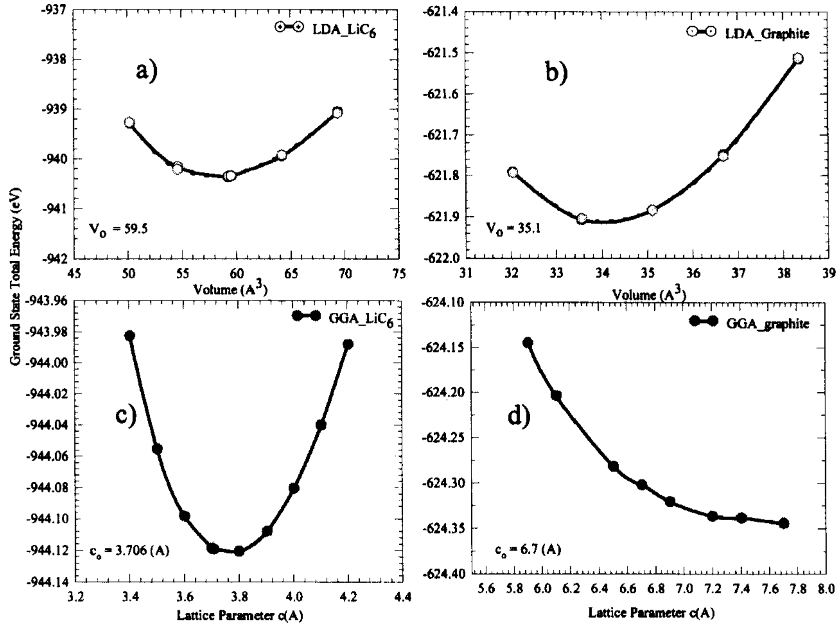

FIGURE 2 (a) and (b) Equation of state for graphite and LiC_6. The total energy calculated within the LDA, is plotted against the volume. (c) A smooth curve fit in a GGA plot of total energy *versus* lattice parameter c for LiC_6 and (d) a plot for graphite. V_o and c_o are experimental values of volume and lattice parameter c respectively. (See Color Plate II).

total-energy calculations were performed as before. We observed an underestimation of graphite and LiC_6 volume by 2.7% and 0.7% respectively. The GGA calculations for graphite underestimated the volume by 3.5%. This is expected, considering the value obtained for the calculations of both lattice parameters a and c for both systems within the two approximations.

Electron Density

The calculated valence electron pseudocharge density of graphite in the (010) plane perpendicular to the graphenes is given in Figures 3a and b for the LDA and GGA respectively. A high concentration of charge is observed between neighbouring carbon atoms suggesting covalent bonding, in agreement with previous LDA results [22]. Generally, charge distributions appear similar for LDA and GGA on this scale. Contour plot of the difference between the LDA and GGA electron density on a similar plane is given in Figure 3c. The magnitude of difference density, ρLDA$-\rho$GGA, is very

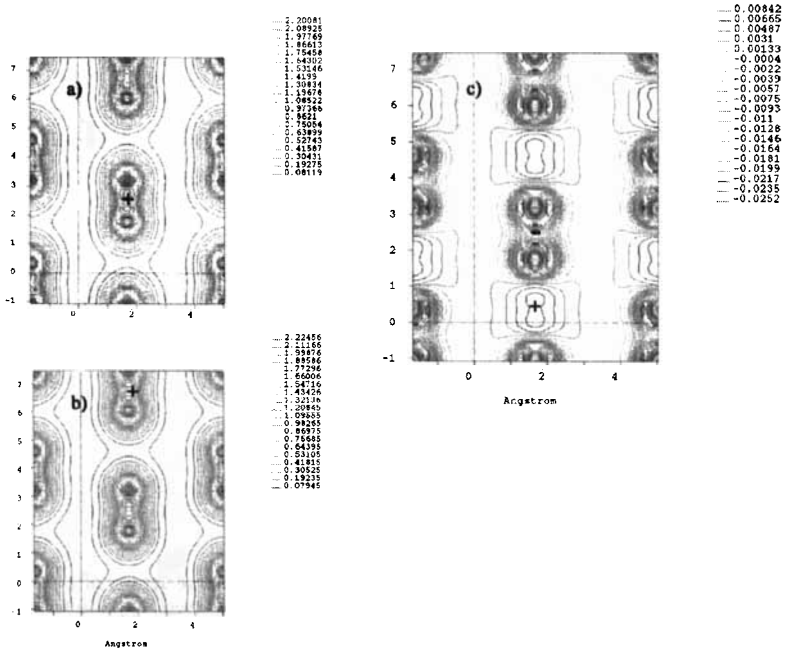

FIGURE 3 Contour plot of the (a) LDA and (b) GGA valence charge density of graphite plotted in a (010) plane which is perpendicular to the graphenes and also features the C—C bond. Contour labels are in units of electrons/Å^3 and varies from −0.02 e/Å^3 to ~2 e/Å^3. (c) the contour plot of the difference between the LDA and GGA valence electron density of graphite, plotted in the same plane. Positive and negative zones of electron density are labeled by + and −, respectively. (See Color Plate III).

small compared with the total electron densities. The regions of positive contour indicate that LDA density is larger in the graphene ring, hence tending to contract the ring. The GGA density has a slightly higher contribution in the bond connecting neighbouring carbon atoms of the graphene ring. LDA charge density is dominant in the weak π-bonding region between layers with no visible trace of GGA charge density. Indeed this explains why, the GGA fails to predict the c lattice parameter in structural calculations.

Contour plots of the LDA and GGA valence pseudocharge density for lithium intercalated graphite plotted in the (100) plane (perpendicular to the graphenes including the C—C bond), are given in Figures 4a and b respectively. The AγAγAγA... stacking sequence is quite apparent and as in graphite, charge distributions for LDA and GGA look the same on this scale. A high charge density is noted along bonds connecting carbon atoms within the graphenes. The lithium ion is located midway between the

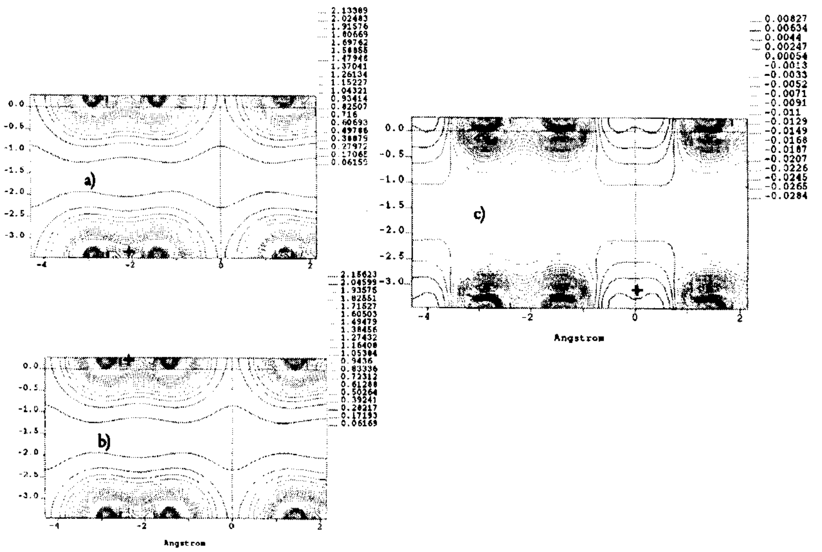

FIGURE 4 Contour plot of the (a) LDA and (b) GGA valence charge density of LiC_6 plotted in a (100) plane which include the lithium ion midway the graphitic layers and also features the C—C bond within the graphenes. Contour labels are in units of electrons/Å^3 and varies from $-0.03\,e/Å^3$ to $\sim 2\,e/Å^3$. (c) Contour plot of the difference between the LDA and GGA valence electron density of LiC_6, plotted in the same plane. Positive and negative zones of electron density are labeled by + and −, respectively. (See Color Plate IV).

graphitic layers, at the carbon ring center. The contour plot of the difference between the LDA and GGA valence pseudodensity for LiC_6, in the (100) plane, is given in Figure 4c. As in graphite the charge density from LDA is larger in the graphene ring. The contours that are associated with this strong LDA contribution are extended into the interplanar region, towards lithium ions, more than in graphite. The GGA charge densities tend to be larger along the C—C bonds as in graphite.

In order to compare the effects of the LDA and GGA on interlayer bonding, we have subtracted the isolated-graphite-layer electronic density from the graphite electronic density. The LDA calculations (Fig. 5a) shows that the electronic charge in the neighbourhood of the α atoms is depleted along the c-axis direction, in agreement with previous results [24]. These electrons are transferred to the neighbourhood of the β atoms, and also between the A and B layers. The latter increase of charge, which extends homogeneously in the entire interplanar region, contributes towards the weak Van der Waals bonding. Consequently, LDA predicts the c lattice parameter of graphite reasonably well, as shown in Table I. For the GGA

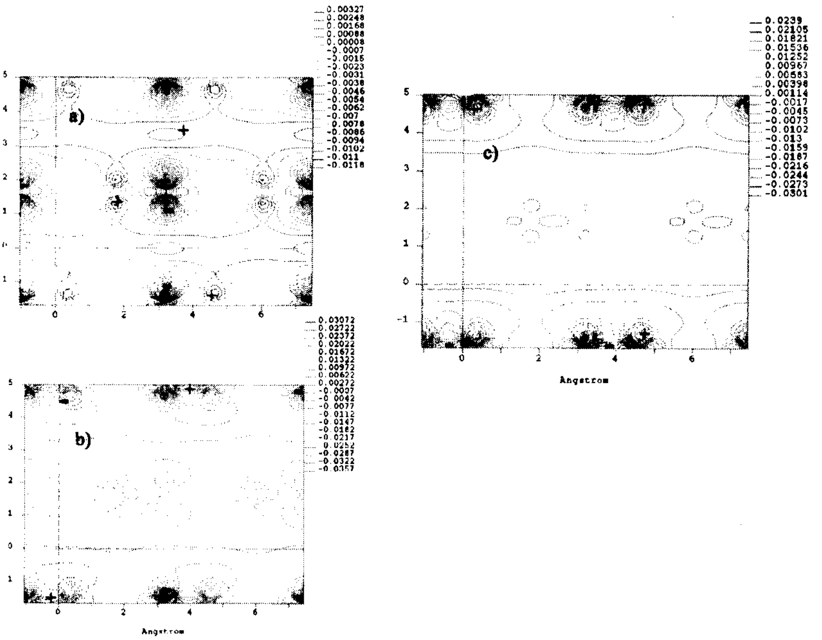

FIGURE 5 Contour plot of the transfer charge due to stacking of graphene layers obtained by the following process: density of graphite minus that of reference graphite layers: A-plane and B-plane. Positive and negative zones of electron density are labeled by + and −, respectively. (a) LDA density difference and (b) GGA density difference while (c) is the difference between (a) and (b) as explained in the discussion. (See Color Plate V).

calculations (Fig. 5b), almost no gain or loss of electrons is shown on α and β atoms in the B layer. A depletion of electrons is shown on both α and β atoms in the A-layer with significant charge residing in the bond between the two atoms. There is no delocalisation of electrons between the **A** and **B** layers, resulting in almost no bonding between the layers. This perhaps explains why GGA fails to predict the c lattice parameter Table I.

Indeed the charge difference between contributions from LDA and GGA (Fig. 5c), confirms that pseudocharge density from LDA are slightly dominant in the interlayer and in the neighbourhood of α and β atoms, particularly in the A-layer. Those of GGA are dominant in the bonds connecting α and β atoms in the A-layer. Although the electron charge densities are three orders of magnitude smaller than those of maximum valence densities, they do, however, provide a preliminary explanation on the sticking of layers as described by the LDA and GGA representations of the exchange correlation energy.

CONCLUSION

We have shown the effects of LDA and GGA on structural and electronic properties of graphite and lithium intercalated graphite. Lattice parameters are generally well reproduced with exception of the c parameter in graphite, which could not be predicted by GGA. It has been noted that this approximation significantly underestimates the weaker π bond between adjacent carbon layers.

Acknowledgment

We would like to acknowledge informative discussion we had at the initial stage of this work with Dr. Eric Wimmer. We are also grateful to the Foundation for Research and Development (FRD) and Royal Society (UK) for financial support.

References

[1] Hohenberg, P. and Kohn, W. (1964). "Inhomogeneous electron gas", *Phys. Rev.*, **136**, B864.

[2] Kohn, W. and Sham, L. (1965). "Self-consistent equations including exchange and correlation effects", *Phys. Rev.*, **140**, A1133.

[3] Perdew, J. P. and Yue, Wang (1986). "Accurate and simple density functional for the electronic exchange energy: Generalized gradient approximation", *Phys. Rev.*, **B33**, 8800; Perdew, J. P. (1986). "Density-functional approximation for the correlation energy of the inhomogeneous electron gas", *Phys. Rev.*, **B33**, 8822.

[4] Becke, A. D. (1986). *J. Chem. Phys.*, **84**, 4524; Becke A. D. (1988). "Density-functional exchange-energy approximation with correct asymptotic behavior", *Phys. Rev.*, **38**, 3098.

[5] Dahn, J. R. *et al.* (1994). "Carbons and Graphites as substitutes for the lithium anode", In: *Lithium Batteries: New Materials, Developments and Perspectives*, Lithium Chemistry Library, Pistoia, G. Ed., Vol. 5, Elsevier, Amsterdam, 1.

[6] Nicklow, R., Wakabayashi, N. and Smith, H. G. (1972). "Lattice dynamics of pyrolytic graphite", *Phys. Rev.*, **B5**, 4951.

[7] Bianconi, Hagstrom, S. B. M. and Bachrach, R. Z. (1977). "Photoemmission studies of graphite high-energy conduction-band and valence-band states using soft-X-rays synchrotron radiation excitation", *Phys. Rev.*, **B16**, 5543.

[8] Zanini, M., Ching, L. Y. and Fischer, J. E. (1978). "Raman scattering in LiC_6. Further evidence for a rigid-band-model interpretation", *Phys. Rev.*, **B18**, 2020.

[9] McGovern, I. T., Eberhardt, W., Plummer, E. W. and Fischer, J. E. (1980). "The bandstructures of graphite and graphite intercalation compounds as determined by angle resolved photoemission using synchrotron radiation", *Physica*, **B99**, 415.

[10] Eberhardt, W., McGovern, I. T., Plummer, E. W. and Fisher, J. E. (1980). "Charge-transfer and non-rigid-band effects in graphite compound LiC_6", *Phys. Rev. Lett.*, **44**, 200.

[11] Wu, N. J. and Ignatiev, A. (1982). "Low-energy-electron-diffraction structural determination of the graphite (0001) surface", *Phys. Rev.*, **B25**, 2983.

[12] Law, A. R. *et al.* (1983). "Angle-resolved photoemission and secondary electron emission from single-crystal graphite", *Phys. Rev.*, **B28**, 5332.

[13] Grunes, L. A. *et al.* (1983). "Valence and core electronic excitation in LiC_6", *Phys. Rev.*, **B28**, 6681.

[14] Fischer, D. A. *et al.* (1991). "Graphitic interlayer states: A carbon *K* near-edge X-ray-absorption fine-structure study", *Phys. Rev.*, **B44**, 1427.

[15] Schinder, T. L. and Vohra, Y. K. (1995). "A micro-Raman investigation of high-pressure quenched graphite", *J. Phys: Condens. Matter*, **L7**, 673.

[16] Boettger, J. C. (1997). "All-electron full-potential calculation of the electronic band structure, elastic constants, and equation of state for graphite", *Phys. Rev.*, **B55**, 11202.

[17] Holzwarth, N. A. W. and Rabii, S. (1977). "Energy band structure of lithium-graphite intercalation compound", *Mat. Sc. Eng.*, **31**, 195.

[18] Holzwarth, N. A. W., Louie, S. G. and Rabii, S. (1983). "Lithium-intercalated graphite: Self-consistent electronic structure for stages one, two, and three", *Phys. Rev.*, **B28**, 1013.

[19] Posternak, M., Baldereschi, A., Freeman, A. J., Wimmer, E. and Weinert, M. (1983). "Prediction of electronic interlayer states in graphite and reinterpreation of alkali bands in graphite intercalation compounds", *Phys. Rev. Lett.*, **50**, 761.

[20] Chen, N. and Rabii, S. (1985). "Theoretical investigation of the optical spectra of LiC$_6$", *Phys. Rev.*, **B31**, 4784.

[21] Chou, M. Y., Cohen, M. L. and Louie, S. G. (1986). "Theoretical compton profiles of graphite and LiC$_6$", *Phys. Rev.*, **B33**, 6619.

[22] Charlier, J. C., Gonze, X. and Michenaud, J. P. (1991). "First-principle study of the electronic properties of graphite", *Phys. Rev.*, **B43**, 4579.

[23] Lang, L., Doyen-Lang, S., Charlier, A. and Charlier, M. F. (1994). "Dynamical study of graphite and graphite intercalation compounds", *Phys. Rev.*, **B49**, 5672.

[24] Charlier, J. C., Gonze, X. and Michenaud, J. P. (1994). "Graphite interplanar bonding: Electronic delocalization and van der Waals interaction", *Europhys. Lett.*, **28**, 403.

[25] Ahuja, R. *et al.* (1997). "Optical properties of graphite from first-principles calculations", *Phys. Rev.*, **B55**, 4999.

[26] Payne, M. C., Teter, M. P., Allan, D. C., Arias, T. A. and Joannopoulos, J. D. (1992). "Iterative minimization techniques for ab initio total-energy calculations: Molecular dynamics and conjugate gradients", *Rev. Mod. Phys.*, **64**, 1045.

[27] Teter, M. P., Payne, M. C. and Allan, D. M. (1989). "Solution of Schrodinger's equation for large systems", *Phys. Rev.*, **B40**, 12255.

[28] Troullier, N. and Martins, J. L. (1991). "Efficient pseudopotential for plane-wave calculations", *Phys. Rev.*, **B43**, 1993; N. Troullier and J. L. Martins (1991). "Efficient pseudopotential for plane-wave calculations. II. Operations for fast iterative diagonalization", *Phys. Rev.*, **B43**, 8861.

[29] Kleinmann, L. and Bylander, D. M. (1982). "Efficacious form for model pseudopotential", *Phys. Rev. Lett.*, **48**, 1425.

[30] Ceperly, D. M. and Adler, B. J. (1980). "Ground state of the electron gas by a stochastic method", *Phys. Rev. Lett.*, **45**, 566.

[31] Perdew, J. P. and Zunger, A. (1981). "Self-interaction correction to density-functional approximations for many-electrons systems", *Phys. Rev.*, **B23**, 5048.

[32] White, J. A. and Bird, D. M. (1994). "Implementation of gradient-corrected exchange-correlation potentials in Car-Parrinello total-energy calculations", *Phys. Rev.*, **B50**, 4954.

[33] Monkhorst, H. J. and Pack, J. D. (1976). "Special points for Brillouin-zone integrations", *Phys. Rev.*, **13**, 5188.